International Journal of Engineering & Technology, 7 (4.30) (2018) 389-392

International Journal of Engineering & Technology

Website: www.sciencepubco.com/index.php/IJET

Research paper

Effect Of Co^{3+} Substitution on Electro-Magnetic Properties of $Pr_{0.75}Na_{0.25}mno_3$ and $Nd_{0.75}Na_{0.25}mno_3$ Manganites

Nurhabibah Nabilah Ab Mannan [1], Sufia Aqilah Razali[2], Suhadir Shamsuddin [3]*, Mohamad Zaky Noh [4], Zakiah Mohamed[5]

[1,2,3,4]*Ceramics and Amorphous Group (CerAm), Faculty of Applied Sciences and Technology, Pagoh Higher Education Hub, Universiti Tun Hussein Onn Malaysia, 84600 Panchor, Johor, Malaysia*

[5]*Faculty of Applied Sciences, Universiti Teknologi MARA, 40450 Shah Alam, Selangor, Malaysia*

**Corresponding author E-mail:suhadir@uthm.edu.my*

Abstract

This paper reports influences of cobalt (Co) substituted at Mn-site of $Pr_{0.75}Na_{0.25}Mn_{1-x}Co_xO_3$ and $Nd_{0.75}Na_{0.25}Mn_{1-y}Co_yO_3$ on structure, electrical transport and magnetic properties. All of the samples were prepared via standard solid state reaction method. X-ray diffraction measurement indicates that all samples were crystallized in an orthorhombic structure (space group *Pnma*). Resistivity measurement displays the $x = 0$ sample manifests an insulator behavior while metal-insulator transition was found at 108 K and 84 K for $x = 0.02$ and 0.05 respectively for $Pr_{0.75}Na_{0.25}Mn_{1-x}Co_xO_3$. On the other hand, all of the samples for $Nd_{0.75}Na_{0.25}Mn_{1-y}Co_yO_3$ showed insulator behavior down to low temperature and analysis of the resistivity change with respect to temperature, $d\ln\rho/dT^{-1}$ versus T reveals a slope changes of resistivity have been recorded. Two obvious peaks were recorded from the analysis for $y = 0.02$ and 0.05 which can be suggested to the existence of charge order transition at the vicinity. For magnetic properties, $x = 0$ sample showed a paramagnetic-antiferromagnetic transition and further substitution of Co, $x = 0.02$ and 0.05, induce the paramagnetic-ferromagnetic transition and antiferromagnetic arrangement respectively. Meanwhile, further substitution of Co, $y = 0.02$ and 0.05 indicate antiferromagnetic transition with increasing T_N as Co increased.

Keywords: *Charge Ordered; Double Exchange Mechanism; Manganites*

1. Introduction

Rare-earth perovskite manganite with the compositional formula of $R_{1-x}A_xMnO_3$ where R is trivalent rare earth and A is divalent alkaline earth ions have caught much interest due to their interesting electrical transport and magnetic properties such as colossal magnetoresistance, charge ordering and metal to insulator behavior [1–5]. In manganite compounds, the coexistence of ferromagnetic to paramagnetic transition at Curie temperature (T_C) and metal to insulator transition temperature at metal-insulator temperature (T_{MI}) are usually interpreted by Zener's double-exchange (DE) mechanism due to the mixed valency of the manganites. This mechanism involves simultaneous hopping of an electron (e_g) from Mn^{3+} to O^{2-} and from O^{2-} to Mn^{4+}if the manganese core spins in parallel alignment are ferromagnetically coupled [6]. However, DE mechanism is insufficient to explain the complex behavior of the manganite compounds and other properties such as Jahn-Teller (JT) effect and charge ordering (CO) were also responsible in providing information [7]. The JT effect can be described as the degeneracy of the e_g and t_{2g} orbitals in Mn^{3+} ions and split into two sublevels due to the crystal field splitting which disturbs the MnO_6 arrangement and favors the localization of e_g electron. The localization of the charge carriers will decrease the mobility of the charge carriers, weakening the DE interaction and metallic behavior is reduced [8–10]. Based on previous study, the existence of CO is always found in the half-doped manganites in which the ratio of Mn^{3+} to Mn^{4+} is 1:1 where the ions arranged themselves in an ordered arrangement reported in several divalent doped manganites such as $La_{0.5}Ca_{0.5}MnO_3$ [11,12], $Pr_{0.5}Ca_{0.5}MnO_3$ [13] and $Nd_{0.5}Ca_{0.5}MnO_3$ [7]. In addition, the existence of CO state also can be observed in monovalent doped manganite. For instance, the charge ordering temperature (T_{CO}) for $Nd_{0.75}Na_{0.25}MnO_3$ and $Pr_{0.75}Na_{0.25}MnO_3$ are recorded approximately at 170 K and 220 K respectively [14,15].

On the other hand, small substitution of magnetic Co^{3+} at the Mn site of the manganese compound is believed to alter the properties due to the modification of Mn^{3+}-O^{2-}-Mn^{4+} network [16–18]. It is well known that cobalt shoes different spin states resulting from the competition between values of crystal field splitting and Hund's coupling energy; low spin states ($t_{2g}^6 e_g^1$ $S = 1$ for Co^{2+} and $t_{2g}^6 e_g^0$ $S = 0$ for Co^{3+}), the intermediate spin state ($t_{2g}^5 e_g^1$ $S = 1$ for Co^{3+} and the high spin state ($t_{2g}^5 e_g^2$ $S = 3/2$ for Co^{2+} and $t_{2g}^4 e_g^2$ $S = 2$ for Co^{3+}) [19]. It is reported magnetic Co substitution can suppress the CO state and revive the insulator to metal transition. Liu et al. also have reported the substitution of Co^{3+} in $Nd_{0.75}Na_{0.25}MnO_3$ caused the suppression of the CO state and induced the ferromagnetic as well as metal to insulator transition. Further substitution of Co^{3+} shows the T_{MI} shifted to lower temperature and the ferromagnetic state is hindered [13]. Besides, the Co substitution on $Nd_{0.5}Sr_{0.5}MnO_3$ also diminished the ferromagnetic-metallic state as reported by Kundu et al. [19] Interestingly, the magnetic Co substitution on monovalent doped manganites have been reported by several studies. Pollert et al. reported Co^{2+} ions

Copyright © 2018 Authors. This is an open access article distributed under the Creative Commons Attribution License, which permits unrestricted use, distribution, and reproduction in any medium, provided the original work is properly cited.

acted as local defects in $Pr_{0.8}Na_{0.2}MnO_3$ and the CO state is suppressed for x = 0.04 due to the enhancement of DE interaction while further increase of Co^{2+} concentration supports ferromagnetic DE interaction [20]. Similar observation also have been reported by Pollert et al. for lower concentration of Co^{2+} (x = 0.04) in $Nd_{0.8}Na_{0.2}Mn_{1-x}Co_xO_3$ [21].

It is suggested that substitution of Co^{3+} for Mn^{3+} decreases the ratio of Mn^{3+} to Mn^{4+} which interrupts the ionic arrangement and alter the physical properties. However, the mechanism behind the role of Co in monovalent doped manganites are still debatable since the reports are still limited. To the best of our knowledge, study on the substitution of Co at the Mn site of $Pr_{0.75}Na_{0.25}MnO_3$ and $Nd_{0.75}Na_{0.25}MnO_3$ compounds have not been reported yet. In this study the effect of Co^{3+} substitution at the Mn site on structural, electrical transport and magnetic properties of $Pr_{0.75}Na_{0.25}Mn_{1-x}Co_xO_3$ ($0\leq x\leq 0.05$) and $Nd_{0.75}Na_{0.25}Mn_{1-y}Co_yO_3$ ($0\leq y\leq 0.05$) have been investigated.

2. Materials and Methods

Two series of polycrystalline samples $Pr_{0.75}Na_{0.25}Mn_{1-x}Co_xO_3$ ($0\leq x\leq 0.05$) and $Nd_{0.75}Na_{0.25}Mn_{1-y}Co_yO_3$ ($0\leq y\leq 0.05$) were synthesized via the solid state reaction method. The stoichiometric amounts of high purity (≥99.99%) Pr_2O_3, Na_2CO_3, MnO_2 and Co_2O_3 for Pr-based and Nd_2O_3, Na_2CO_3, MnO_2 and Co_2O_3 for Nd-based were mixed, ground and calcined at 1000 °C for 24 hours followed by several intermediate grindings. The powders were pressed into pellets and sintered at 1200 °C for 24 hours after the final grinding. The phase of the samples was characterized by X-ray diffraction (XRD) technique employing a Bruker D8 Advance at room temperature with Cu-Kα radiation which were operated at 40 kV and 40 mA. The peaks obtained have been analysed by X'Pert HighScore program which were identified from the International Centre for Diffraction Data (ICDD) database. The electrical transport behaviour was carried out by the standard four-point probe technique by increasing the temperature starting from 25 K to 300 K in a Janis model CCS 350ST cryostat without magnetic field. The measurement of AC magnetic susceptibility were carried out utilizing a CryoBIND-T system in conjunction with a SR830 lock-in-amplifier and an oscillator at 240 Hz in the temperature range of 50 K to 300 K.

3. Results and Discussion

3.1. Structural analysis

The XRD patterns of the synthesized $Pr_{0.75}Na_{0.25}Mn_{1-x}Co_xO_3$ ($0\leq x\leq 0.05$) samples at room temperature are shown in Figure 1. All of the samples are crystallized into orthorhombic structure with *Pnma* space group which reliable with the structure as reported from the previous study [22].

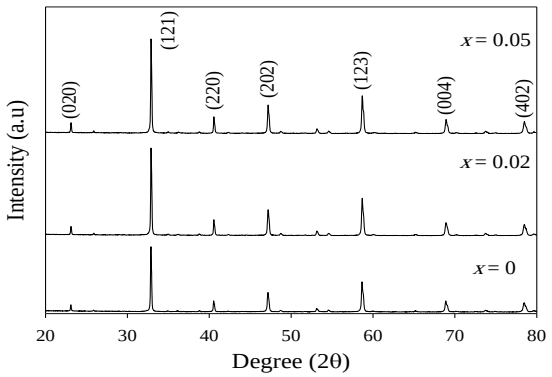

Fig. 1: XRD patterns for $Pr_{0.75}Na_{0.25}Mn_{1-x}Co_xO_3$ ($0\leq x\leq 0.05$).

Table 1 indicates the values of the lattice parameters and unit cell volume (V) of each samples. It can be seen from the table that lattice parameters decrease with the increasing Co content. The decrease of the V also is assumed to be due to the substitution of smaller Co^{3+} (0.61 Å) for Mn^{3+} (0.645 Å) [23]. Besides, the decreasing value of V also is supposed due to conversion of Mn^{3+} into Mn^{4+} (0.53 Å) as substitution of ions at the Mn site disturbs the Mn^{3+}-O^{2-}-Mn^{4+} directly [24].

Table 1: Lattice parameters and unit cell volume of $Pr_{0.75}Na_{0.25}Mn_{1-x}Co_xO_3$ ($0\leq x\leq 0.05$).

Sample	Lattice parameters			V (Å)^3 ±0.1
	a (Å) ±0.001	b (Å) ±0.002	c (Å) ±0.001	
x = 0	5.446	7.696	5.445	228.2
x = 0.02	5.444	7.690	5.443	227.9
x = 0.05	5.443	7.680	5.444	227.6

On the other hand, the X-ray patterns conducted at room temperature of all the $Nd_{0.75}Na_{0.25}Mn_{1-y}Co_yO_3$ ($0\leq y\leq 0.05$) samples are shown in Figure 2. All the diffractograms were indexed to the orthorhombic structure with *Pnma* space group which agrees to the previous report [25]. Table 2 shows the value of lattice parameters and V of each Co substituted in Nd-based. The lattice parameters and V seems to be decreased with increasing of Co^{3+} content which can be suggested due to the successful replacement of Co^{3+} that having smaller ionic radius into Mn site in the lattice structure [26].

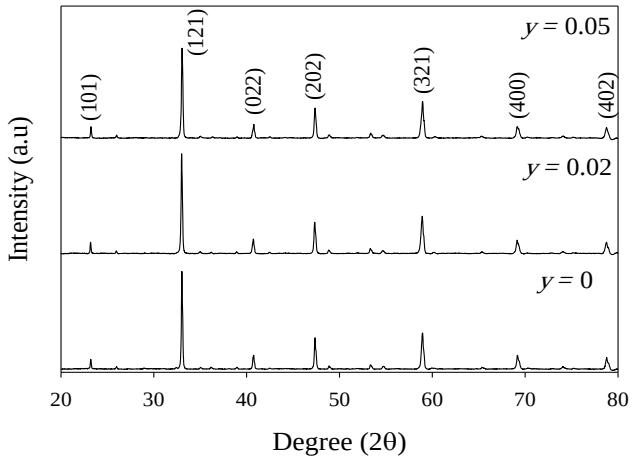

Fig. 2: XRD patterns for $Nd_{0.75}Na_{0.25}Mn_{1-y}Co_yO_3$ ($0\leq y\leq 0.05$).

Table 2: Lattice parameters and unit cell volume of $Nd_{0.75}Na_{0.25}Mn_{1-y}Co_yO_3$ ($0\leq y\leq 0.05$).

Sample	Lattice parameters			V (Å)^3 ±0.1
	a (Å) ±0.001	b (Å) ±0.002	c (Å) ±0.001	
y = 0	5.522	7.670	5.431	230.0
y = 0.02	5.417	7.649	5.413	224.3
y = 0.05	5.403	7.640	5.400	222.9

3.2. Electrical transport properties

Figure 3 depicts the resistivity versus temperature, ρ(T), plot of the $Pr_{0.75}Na_{0.25}Mn_{1-x}Co_xO_3$ samples. It is evident from this plot that x = 0 sample displayed an insulating behaviour over the temperature range as there is no distinct peak indicating the absence of MI transition. Further substitution of Co^{3+}, x = 0.02 and x = 0.05 samples showed a distinct metal-insulator transition at 108 K and 84 K respectively suggestively due to the DE mechanism. Meanwhile, the shifting of MI transition to lower temperature as increasing Co^{3+} concentration could be assumed due to replacements of Co ions at Mn site and cause the depletion of the Mn ion ratio,

hence weakening the DE mechanism and contributes to the destruction of long range ferromagnetic order [25,27,28].

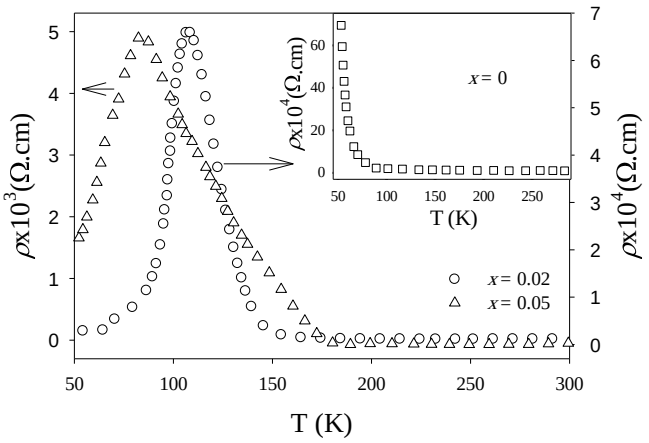

Fig. 3: Temperature dependence of electrical resistivity of $Pr_{0.75}Na_{0.25}Mn_{1-x}Co_xO_3$ ($0 \le x \le 0.05$).

Figure 4 shows the temperature dependence of the electrical resistivity for the $Nd_{0.75}Na_{0.25}Mn_{1-y}Co_yO_3$ ($0 \le y \le 0.05$) samples. All of the samples showed an insulating transport behavior over the temperature range. An indistinct slope of change was observed below 200 K and a plot of $dln\rho/dT^{-1}$ vs T was constructed around the vicinity of temperature as indicated in inset of Figure 4. Two distinct peaks were observed clearly at temperature around 200 K and 235 K for y = 0.02 and y = 0.05 samples respectively from the analysis of $dln\rho/dT^{-1}$ vs T curve (Inset Figure 4). Such observation can be suggested due to the existing of CO state as the peaks located in the of the charge ordering transition temperature

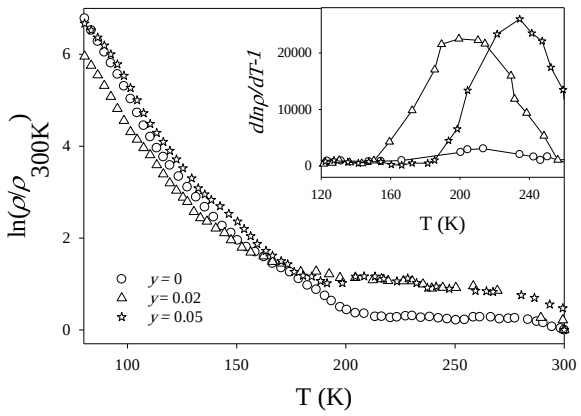

[29].

Fig. 4: Temperature dependence of electrical resistivity of $Nd_{0.75}Na_{0.25}Mn_{1-y}Co_yO_3$ ($0 \le y \le 0.05$). Inset is $d\ln\rho/dT^{-1}$ vs. T for $Nd_{0.75}Na_{0.25}Mn_{1-y}Co_yO_3$.

3.3. Magnetic properties

Figure 5 illustrates the effects of the Co substitution on the temperature dependence of AC susceptibility for $Pr_{0.75}Na_{0.25}Mn_{1-x}Co_xO_3$ ($0 \le x \le 0.05$) samples within the temperature range of 50 K – 300 K. The unsubstituted (x = 0) sample exhibits paramagnetic behavior at high temperature and followed by antiferromagnetic transition defined by a declined in χ around T_N ~ 134K. The T_N recorded for this sample was lower compared to the previous report which was stated at around 180 K [30]. The differences between the obtained T_N in this study and as reported by other researcher can be assumed by the microstructure effect of the sample as reported by other researchers [31,32]. On the other hand, paramagnetic to ferromagnetic transition was observed for sample x = 0.02. The T_C value was determined from the temperature corresponding to the minimum value from the derivative of susceptibility ($d\chi/dT$) vs temperature curve. The analysis of $d\chi/dT$ vs T for x = 0.02 sample revealed the T_C approximately at ~ 120 K as indicated in inset of Figure 5. Such observation can be suggested due to the DE mechanism arised from the ratio of Mn^{3+} and Mn^{4+} [33]. However, the substitution of Co for x = 0.05 unveiled the paramagnetic-antiferromagnetic transition along the temperature range with T_N approximately at 113 K. This can be suggested due to the weakening of DE interaction and superexchange antiferromagnetic interaction takes place down the temperature range [34].

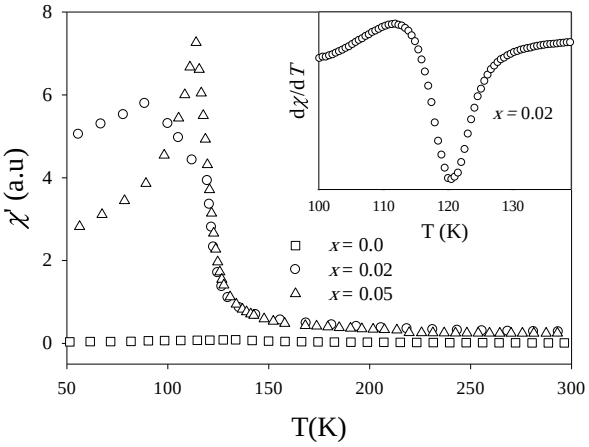

Fig. 5: Temperature dependence of AC susceptibility of $Pr_{0.75}Na_{0.25}Mn_{1-x}Co_xO_3$ with (x = 0, 0.02 and 0.05). Inset is $d\chi/dT$ vs T for $Pr_{0.75}Na_{0.25}Mn_{0.98}Co_{0.02}O_3$.

Figure 6 shows the temperature dependence of AC susceptibility of $Nd_{0.75}Na_{0.25}Mn_{1-y}Co_yO_3$ with (y = 0, 0.02 and 0.05). The presence of CO was observed approximately at 170 K as indicated in the inset of Figure 6 which agreed with previous study [35]. The y = 0 sample exhibits paramagnetic behavior as the temperature decreased. Further substitution of Co at the level of y = 0.02 and 0.05 induce the antiferromagnetic transition with T_N ~ 101 K and 108 K respectively. This can be explained by assuming the superexchange interaction takes place as the concentration of Co^{3+} increased [36]. The increasing values of T_N pointed to the possibility of enhancing the charge ordered state as CO always linked to the antiferromagnetic interaction and this result complied with increasing values of so-called T_{CO} in electrical resistivity data.

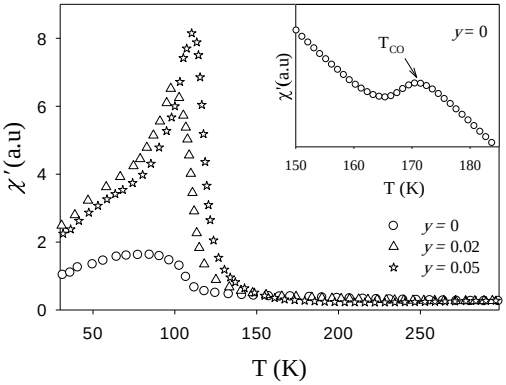

Fig. 6: Temperature dependence of AC susceptibility of $Nd_{0.75}Na_{0.25}Mn_{1-y}Co_yO_3$ with (y = 0, 0.02 and 0.05). Inset in the enlargement data of temperature dependence of AC susceptibility for y = 0.

4. Conclusion

In conclusion, the influence of magnetic Co^{3+} at Mn site for $Pr_{0.75}Na_{0.25}Mn_{1-x}Co_xO_3$ ($0 \le x \le 0.05$) and $Nd_{0.75}Na_{0.25}Mn_{1-y}Co_yO_3$ ($0 \le y \le 0.05$) on structure, electrical transport and magnetic properties have been investigated. From the study conducted, both compounds, $Pr_{0.75}Na_{0.25}Mn_{1-x}Co_xO_3$ and $Nd_{0.75}Na_{0.25}Mn_{1-y}Co_yO_3$ were indexed to orthorhombic structure with *Pnma* space group. For

electrical transport, for $Pr_{0.75}Na_{0.25}Mn_{1-x}Co_xO_3$, the decreasing value of T_{MI} as the Co concentration increased were suggested due to the weakening of DE interaction. Meanwhile, analysis of $dln\rho/dT^{-1}$ vs T from the resistivity measurement for $Nd_{0.75}Na_{0.25}Mn_{1-y}Co_yO_3$ reveals two obvious peaks at 200 K and 235 K for y = 0.02 and 0.05 respectively indicating the probability of the existence of CO state in the samples. For magnetic properties, the x = 0 sample exhibits paramagnetic followed by antiferromagnetic arrangement and paramagnetic-ferromagnetic transition was observed for x = 0.02 which was suggestively due to the enhancement of DE mechanism. On the other hand, the inducement of antiferromagnetic arrangement was observed for y = 0.02 and y = 0.05 with T_N ~ 101 K and 108 K respectively.

Acknowledgement

This work was supported by the Ministry of Education (MOE) of The Federal Government of Malaysia-Putrajaya under Fundamental Research Grant Scheme (FRGS) vot 1597 and partly sponsored by Centre of Graduate Studies, UTHM.

References

[1] Moure C & Peña O, Magnetic features in REMeO3 perovskites and their solid solutions (RE=rare-earth, Me=Mn, Cr), Journal of Magnetism and Magnetic Materials, Vol. 337–338, (2013), pp. 1–22.

[2] Rao CNR & Subba Rao GV, Electrical conduction in metal oxides, Physica Status Solidi (a), Vol. 1, No. 4, (1970), pp. 597–652.

[3] Meadowcroft D, Low-cost oxygen electrode material, Nature, Vol. 226, No. 5248, (1970), pp. 847–848.

[4] Zhang T, Wang XP, Fang QF & Li XG, Magnetic and charge ordering in nanosized manganites, Applied Physics Reviews, Vol. 1, No. 3, (2014), pp. 031302.

[5] Rahmouni H, Dhahri A & Khirouni K, The effect of tin addition on the electrical conductivity of Sn-doped LaBaMnO3, Journal of Alloys and Compound., Vol. 591, (2014), pp. 259–262.

[6] Zener C, Interaction between the d-shells in the transition metals. II. Ferromagnetic compounds of manganese with perovskite structure, Phyical. Review, Vol. 82, No. 3, (1951), pp. 403–405.

[7] Shamsuddin S, Abdel-Baset MA Ibrahim & Yahya AK, Effects of Cr substitution and oxygen reduction on elastic anomaly and ultrasonic velocity in charge-ordered Nd0.5Ca0.5Mn1-xCrxO3-δ ceramics, Ceramics Internationa, Vol. 39, (2013), pp. S185–S188.

[8] Millis AJ, Boris I. Shraiman & Mueller R, Dynamic Jahn-Teller Effect and Colossal Magnetoresistance in La1-xSrxMnO3., Physical. Review Letters, Vol. 77, No. 1, (1996), pp. 175–178.

[9] Roy S & Ali N, Charge transport and colossal magnetoresistance phenomenon in La1-xZrxMnO3, Journal of Applied Physics, Vol. 89, No. 11, (2001), pp. 7425–7427.

[10] Das S, Poddar A, Roy B & Giri S, Studies of transport and magnetic properties of Ce-doped LaMnO3, Journal of Alloys Compound., Vol. 365, No. 1–2, (2004), pp. 94–101.

[11] Walha I, Ehrenberg H, Fuess H & Cheikhrouhou A, Structure and magnetic properties of lanthanum and calcium-deficient La0.5Ca0.5MnO3 manganites, Journal of Alloys Compdounds, Vol. 433, (2007), pp. 63–67.

[12] Awana VPS, Tripathi R, Balamurugan S, Kumar A, Dogra A & Kishan H, Thermal hysteresis in electrical transport of charge ordered La0.5Ca0.5MnO3 manganites, Journal of Alloys and Compounds, Vol. 475, (2009), pp. L13–L16.

[13] Liu Y, Kong H & Zhu C, Coexistence of charge ordering and ferromagnetism in Nd0.5Ca0.5Mn1-xCoxO3 ($x \leq 0.1$), Journal of Alloys and Compounds, Vol. 439, (2007), pp. 33–36.

[14] Lakshmi YK & Reddy PV, Investigation of ground state in sodium doped neodymium manganites, Physics Letter A, Vol. 375, (2011), pp. 1543–1547.

[15] Li Y, Mao J, Sui Y, Wang X, Zhang W, Liu Y, Zhu R & Su W, Synthesis, structural and transport properties of Pr0.75Na0.25Mn1-xFexO3 ($0.0 \leq x \leq 0.3$), Journal of Alloys and Compounds, Vol. 441, (2007), pp. 1–5.

[16] Dutta P, Das D, Chatterjee S & Majumdar S, Effect of Co doping on magneto-transport properties of Eu0.5Sr0.5MnO3, Journal of Alloys and Compounds, Vol. 590, (2014), pp. 313–317.

[17] Xu X, Li Y, Hou F, Cheng Q & Su R, Effect of Co substitution on magnetic ground state in Sm0.5Ca0.5MnO3, Journal of Alloys and Compounds, Vol. 628, (2015), pp. 89–96.

[18] Huang X, Chen W, Wu W, Zhou Y, Wu J, Wang Q & Chen Y, Effect of Co3+ substitution on the structure and magnetic properties of La0.6Ca0.4MnO3, Journal of Material Science: Materials in Electronics, Vol. 27, No. 5, (2016), pp. 5395–5402.

[19] Kundu S & Nath TK, Effect of Mn doping on magnetic and transport properties of Nd0.5Sr0.5Co(1-y)MnyO3, Journal of Magnetism and Magnetic Materials, Vol. 325, (2013), pp. 1–6.

[20] Pollert E, Hejtmánek J, Jirák Z, Knížek K & Maryško M, Influence of Co doping on properties of Pr0.8Na0.2Mn(1-y)CoyO3 perovskites, Vol. 174, (2003), pp. 466–470.

[21] Pollert E, Hejtmánek J, Jirák Z, Knížek K, Maryško M, Grenier JC & Etourneau J, Insulator-metal transition in Nd0.8Na0.2Mn(1-x)CoxO3 perovskites, Journal of Solid State Chemistry, Vol. 170, (2003), pp. 368–373.

[22] M'nassri R, Khelifi M, Rahmouni H, Selmi A, Khirouni K, Chniba-Boudjada N & Cheikrouhou A, Study of physical properties of cobalt substituted Pr0.7Ca0.3MnO3, Ceramics International, Vol. 42, No. 5, (2016), pp. 6145-6153.

[23] Gritzner G, Ammer J, Kellner K, Kavečansky V & Zentková M Preparation, structure and properties of La0.67Pb0.33(Mn1-xCox-)O3-δ, Applied Physics A, Vol. 365, No 2, (2008), pp. 359–365.

[24] Troyanchuk IO, Khomchenko VA, Chobot GM, Kurbakov AI, Vasil'ev AN, Eremenko VV, Sirenko VA, Szymczak H & Szymczak R, Spin-reorientational transitions in low-doped Nd(1- x)CaxMnO3 manganites: the evidence of an inhomogeneous magnetic state, Journal of Physics: Condensed Matter, Vol. 15, No 50, (2003), pp. 8865–8880.

[25] Abdullah H & Halim SA, Disorder Phenomena in Nd-doped (Pr1-xNdx)0.67Ba0.33MnO3 manganites, Vol. 39, No. 1, (2010), pp. 93–98.

[26] Shannon RD, Revised effective ionic radii and systematic studies of interatomic distances in halides and chalcogenides, Acta Crystallographica, Vol. 32, No. 5, (1976), pp. 751-767.

[27] Jie Y & Yuping S, Study of doping effect , phase separation and heterojunction in CMR manganites, Vol. 56, No. 1, (2013), pp. 85–98.

[28] Varshney D, Mansuri I, Shaikh MW & Kuo YK, Effect of Fe and Co doping on electrical and thermal properties of La0.5Ce0.5Mn1-x(Fe, Co)xO3 manganites, Materials Research Bulletin, Vol. 48, No. 11, (2013), pp. 4606–4613.

[29] Shamsuddin S, Supardan SN, Abdel-Baset MA Ibrahim & Yahya AK, Ultrasonic anomaly near the charge ordering transition in Sr-doped Nd0.3La0.2Ca0.5-xSrxMnO3 manganites, Journal of Superconductivity and Novel Magnetism, Vol. 27, No. 5, (2014), pp. 1229–1234.

[30] Satoh T, Kikuchi Y, Miyano K, Pollert E, Hejtmánek J & Jirák Z, Irreversible photoinduced insulator-metal transition in the Na-doped manganite Pr0.75Na0.25MnO3, Physical Review B, Vol. 65, (2002), pp. 125103.

[31] Kameli P, Salamati H & Aezami A, Influence of grain size on magnetic and transport properties of polycrystalline La0.8 Sr0.2 MnO3 manganites, Journal of Alloys and Compounds, Vol. 450, (2008), pp. 7–11.

[32] Dey P & Nath TK, Effect of grain size modulation on the magneto- and electronic-transport properties of La0.7Ca0.3MnO3 nanoparticles: The role of spin-polarized tunneling at the enhanced grain surface, Physical Review B, Vol. 73, (2006), pp. 214425.

[33] Shi JB, Wu FC & Lin CT, Electrical transport , magnetism , and magnetoresistance in La0.7Sr0.3(Mn1-xCox)O3, Applied Physics A, Vol. 68, No. 5, (1999), pp. 577–581.

[34] Srivastava SK & Ravi S, Magnetic properties of transition metal substituted La0.85Ag0.15Mn1-yMyO3 compounds (M=Co, Cr and Al), Journal of Magnetism and Magnetic Materials, Vol. 321, No. 24, (2009), pp. 4072–4080.

[35] Li ZQ, Zhang XH, Li WR, Song W, Liu H, Wu P, Bai HL & Jiang EY, Charge ordering, magnetic, electrical transport and thermal transport properties of Nd0.75 Na0.25MnO3 manganite, Physica B, Vol. 371, pp. 177–181.

[36] Bitla Y, Kaul SN, Barquín LF, Gutiérrez J, Barandiarán JM, & Peña A, Observation of isotropic-dipolar to isotropic-Heisenberg crossover in Co-and Ni-substituted manganites, New Journal of Physics, Vol. 12, (2010), pp. 1-23.